



HAL
open science

Mathematical model for coupling a quasi-unidimensional perfect flow with an acoustic boundary layer

Régis Msallam, François Dubois

► **To cite this version:**

Régis Msallam, François Dubois. Mathematical model for coupling a quasi-unidimensional perfect flow with an acoustic boundary layer. 2002. hal-00491417

HAL Id: hal-00491417

<https://hal.science/hal-00491417>

Preprint submitted on 11 Jun 2010

HAL is a multi-disciplinary open access archive for the deposit and dissemination of scientific research documents, whether they are published or not. The documents may come from teaching and research institutions in France or abroad, or from public or private research centers.

L'archive ouverte pluridisciplinaire **HAL**, est destinée au dépôt et à la diffusion de documents scientifiques de niveau recherche, publiés ou non, émanant des établissements d'enseignement et de recherche français ou étrangers, des laboratoires publics ou privés.

Mathematical model for coupling a quasi-unidimensional perfect flow with an acoustic boundary layer

Régis Msallam [◇] and François Dubois ^{*}

July 26, 1999, revised version June 12, 2002. [†]

Abstract

Nonlinear acoustics of wind instruments conducts to study unidimensional fluid flows. From physically relevant approximations that are modeled with the thin layer Navier Stokes equations, we propose a coupled model where perfect fluid flow is described by the Euler equations of gas dynamics and viscous and thermal boundary layer is modeled by a linear equation. We describe numerical discretization, validate the associated software by comparison with analytical solutions and consider musical application of strongly nonlinear waves in the trombone.

[◇] Institut de Recherche et de Coordination Acoustique / Musique,
1 place Stravinsky, F-75004 Paris, France ; Regis.Msallam@ircam.fr

^{*} Applications Scientifiques du Calcul Intensif, bât. 506, BP 167, F-91 403
Orsay Cedex, Union Européenne ; dubois@asci.fr.

[†] Rapport n° 326-99 de l'Institut Aéro Technique du Conservatoire National
des Arts et Métiers à Saint Cyr l'Ecole. Edition du 10 juin 2010.

Résumé

L'acoustique non linéaire des instruments à vents conduit à étudier les écoulements filaires monodimensionnels. À partir d'approximations physiquement réalistes qui sont prises en compte par les équations de Navier Stokes de couche mince, nous proposons un modèle couplé où le fluide parfait est décrit par les équations d'Euler de la dynamique des gaz et le fluide visqueux et conducteur de chaleur par une équation linéaire de couche limite. Nous détaillons la discrétisation numérique retenue et validons le logiciel développé grâce à des solutions analytiques avant d'aborder l'application musicale à la propagation d'ondes fortement non linéaires dans le trombone.

Key words : fluid mechanics, nonlinear acoustics, Euler equations, boundary layer, finite differences.

Contents

1) Introduction	2
2) Thin Layer Navier Stokes equations	3
3) Perfect fluid for main flow	10
4) Acoustic boundary layer	13
5) The coupled problem	14
6) Generalization to axisymmetric geometry	17
7) Numerical approximation of the coupled problem	20
8) First test cases	27
9) Conclusion, acknowledgments	35
10) References	35

1) Introduction.

- In this paper, we study simple models of nonlinear acoustic flows in cylindric or axisymmetric ducts. Our objective is to take into account several physical effects such compressibility of the air, viscous dissipation and thermal conduction, especially in the vicinity of the wall. We consider the flow of a newtonian compressible fluid in a two-dimensional pipe. In a first approximation, the variation of physical fields in the transverse direction can be neglected and an appropriate physical model for such a flow is given by unidimensional equations of gas dynamics (see, *e.g.* Landau-Lifschitz [LL53]). This model is appropriate for the description of

nonlinear waves in shock dynamics (see *e.g.* Courant-Friedrichs [CF48]) and also for weaker waves in nonlinear acoustics (Whitham [Wh74]). Nevertheless, such a model neglects all phenomena that can appear in the boundary layer.

- The boundary layer is the region located near the wall (at a distance of the order of the boundary layer thickness δ) where viscous dissipation and thermal conduction have to be considered. The important role of the boundary layer in duct acoustics has been studied by Chester [Ch64]. Usually, linearized boundary layer equations are considered and the associated mathematical model is the heat equation whose solution can be explicitated using a convolution kernel in time.

- In the domain of acoustics, nonlinear and dissipative effects are usually taken into account via generalized Burgers equations as suggested by Blackstock [Bl85] ; this scalar model contains a source term which is, in the case of ducts, a convolution kernel giving an explicit solution of the linear model of acoustic boundary layer. We refer to Makarov-Ochmann [MO97] for a review of the fundamental results.

- We here focus on the fact that the modelling of an acoustic flow in a pipe can be conducted as a coupling between a perfect fluid and a boundary layer. We refer to Le Balleur [LB80], Zeytounian [Ze92] and Aupoix-Brazier-Cousteix [ABC92] for classical approaches developed in the context of aerodynamics applications. In this paper, we have been inspired by these coupling techniques for pipe flow problem in nonlinear acoustics.

2) Thin Layer Navier Stokes equations.

- We consider the geometry of a two-dimensional pipe of characteristic longitudinal length equal to L . The thickness of the duct is $2h$ and our basic hypothesis is that the ratio $\frac{h}{L}$ is small :

$$(2.1) \quad \frac{h}{L} \ll 1.$$

We consider also some longitudinal length Λ and some length l in the transverse direction ($0 < l \leq h$) that are used for the adimensionalization of the equations (see Figure 1). We distinguish between the two types of flows associated to aerodynamics and acoustics applications.

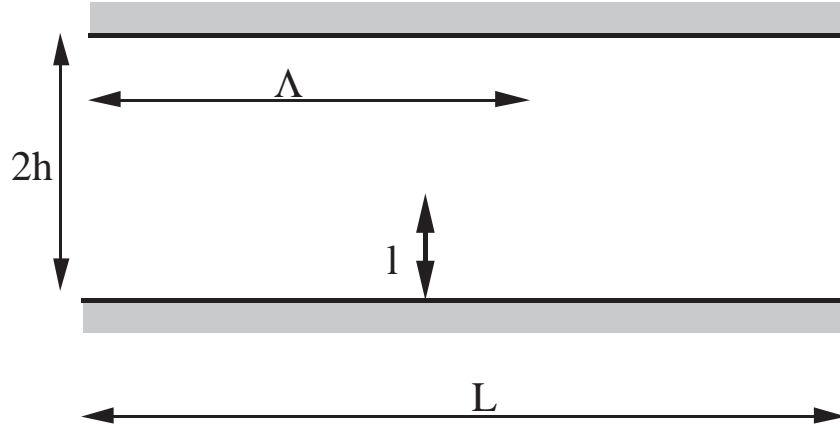


Figure 1 Channel with characteristic lengths.

- In aerodynamics, we suppose simply :

$$(2.2) \quad \Lambda = L.$$

Moreover, the distance l is a distance characteristic of the maximum of the boundary layer thickness (see *e.g.* Schlichting [Sc55]) :

$$(2.3) \quad l = 5 \sqrt{\frac{\mu L}{\rho U}}.$$

In previous expression, ρ , μ and U are respectively the density, the viscosity and the amount velocity of the flow and we introduce also the so-called Reynolds number in aerodynamics :

$$(2.4) \quad R_e^{\text{aero}} = \frac{\rho U L}{\mu}.$$

We note that for extremely thin pipes, the boundary layer occupies all the duct, that is $l \simeq h$. In all cases, we suppose that

$$(2.5) \quad \epsilon \equiv \frac{l}{\Lambda} \approx \frac{1}{\sqrt{R_e^{\text{aero}}}} \ll 1.$$

- In acoustics, if condition

$$(2.6) \quad \frac{h}{\lambda} < \frac{1}{4}$$

is satisfied, the waves propagate only along the axial direction (Pierce [Pi81], see also Bruneau [Br98]) and it is natural to consider the length wave λ as a reference length for the axial direction. We set :

$$(2.7) \quad \Lambda = \lambda.$$

On the other hand, distance l is the natural length constructed from viscosity coefficient μ , density of the air ρ_0 and sound celerity c_0 at usual thermodynamic

conditions for pressure and temperature : $p_0 = 1$ atmosphere and $T_0 = 300$ Kelvins. We set

$$(2.8) \quad l = \frac{\mu}{\rho_0 c_0}$$

and we introduce also the acoustic Reynolds number R_e^{acou} defined similarly to expression (2.4) :

$$(2.9) \quad R_e^{\text{acou}} = \frac{\rho_0 c_0 \lambda}{\mu}.$$

The ratio $\frac{l}{\Lambda}$ between right hand sides of expressions (2.8) and (2.7) satisfies the following hypothesis :

$$(2.10) \quad \epsilon \equiv \frac{l}{\Lambda} \approx \frac{1}{R_e^{\text{acou}}} \ll 1.$$

In practice, $l \simeq 10^{-8} m$ and if the frequency of the acoustic wave (with wave length λ) is less than 1 Ghz, condition (2.10) is satisfied. More precisely, we set with Bruneau, Herzog, Kergomard and Polak [BHKP89],

$$(2.11) \quad l_{vh} = \left(\frac{4}{3} \mu + \mu_v \right) \frac{1}{\rho_0 c_0} + (\gamma - 1) \frac{k}{\rho_0 c_0 C_p}$$

where μ_v is the volumic viscosity, $\gamma = 7/5$ is the ratio of specific heats, k the thermic conductivity and C_p the calorific capacity at constant pressure. In the air the volumic viscosity μ_v is negligible compared to viscosity μ and $(\gamma - 1) k / C_p$ is of the order of viscosity μ *i.e.* the Prandtl number (see *e.g.* Schlichting [Sc55]) is of the order of 1. Therefore,

$$(2.12) \quad l \approx l_{vh}.$$

that enforces hypothesis (2.8).

- The flow is supposed to satisfy the Navier Stokes equations of conservation of mass, impulse and energy. Recall that the unknowns are density ρ , velocity (u, v) , pressure p and internal specific energy e . The thermodynamic variables are supposed to satisfy the state equation for the air that takes the classical form of a perfect gas equation

$$(2.13) \quad p = (\gamma - 1) \rho e.$$

In the following, we neglect the volumic viscosity μ_v and assume that the Stokes hypothesis concerning the two viscosities is valid. In consequence, the classical analytic expression of the Navier-Stokes equations (*e.g.* Landau and Lifschitz [LL53]) takes the form

$$(2.14) \quad \frac{\partial \rho}{\partial t} + \frac{\partial}{\partial x}(\rho u) + \frac{\partial}{\partial y}(\rho v) = 0$$

$$(2.15) \quad \frac{\partial}{\partial t}(\rho u) + \frac{\partial}{\partial x}(\rho u^2 + p) + \frac{\partial}{\partial y}(\rho u v) = \mu \left[\frac{\partial}{\partial x} \left(\frac{4}{3} \frac{\partial u}{\partial x} + \frac{1}{3} \frac{\partial v}{\partial y} \right) + \frac{\partial^2 u}{\partial y^2} \right]$$

$$(2.16) \quad \frac{\partial}{\partial t}(\rho v) + \frac{\partial}{\partial x}(\rho u v) + \frac{\partial}{\partial y}(\rho v^2 + p) = \mu \left[\frac{\partial^2 v}{\partial x^2} + \frac{\partial}{\partial y} \left(\frac{1}{3} \frac{\partial u}{\partial x} + \frac{4}{3} \frac{\partial v}{\partial y} \right) \right]$$

$$(2.17) \quad \left\{ \begin{array}{l} \frac{\partial}{\partial t} \left(\rho \left(e + \frac{1}{2} (u^2 + v^2) \right) \right) + \frac{\partial}{\partial x} \left(\rho u \left(e + \frac{1}{2} (u^2 + v^2) \right) + p u \right) + \\ + \frac{\partial}{\partial y} \left(\rho v \left(e + \frac{1}{2} (u^2 + v^2) \right) + p v \right) = \\ = \mu \frac{\partial}{\partial x} \left[u \left(\frac{4}{3} \frac{\partial u}{\partial x} - \frac{2}{3} \frac{\partial v}{\partial y} \right) + v \left(\frac{\partial u}{\partial y} + \frac{\partial v}{\partial x} \right) \right] + \\ + \mu \frac{\partial}{\partial y} \left[u \left(\frac{\partial v}{\partial x} + \frac{\partial u}{\partial y} \right) + v \left(\frac{4}{3} \frac{\partial v}{\partial y} - \frac{2}{3} \frac{\partial u}{\partial x} \right) \right] + k \left(\frac{\partial^2 T}{\partial x^2} + \frac{\partial^2 T}{\partial y^2} \right). \end{array} \right.$$

• We detail the way we adimensionalize the Navier Stokes equations. First we have two length scales Λ and l for longitudinal and transverse directions respectively ; we denote by \bar{x} and \bar{y} these two space variables without dimension :

$$(2.18) \quad \bar{x} = \frac{x}{\Lambda}$$

$$(2.19) \quad \bar{y} = \frac{y}{l}.$$

Second, we introduce some longitudinal reference velocity U . This velocity defines a time reference τ and an adimensionalized time \bar{t} according to

$$(2.20) \quad \tau = \frac{\Lambda}{U}$$

$$(2.21) \quad \bar{t} = \frac{t}{\tau}.$$

If $\Lambda = \lambda$ is the length wave and $U = c_0$ is a typical choice for the adimensionalization of velocity in acoustics, then τ is the period of the wave, *i.e.* the time for the acoustic perturbation to travel one length wave. We introduce a second reference velocity V associated to this time τ and the transverse distance l :

$$(2.22) \quad V = \frac{l}{\tau}.$$

If a particle travels distance Λ with axial velocity U during time τ , it travels distance l with transverse velocity V during the same time interval. Therefore, we define dimensionless velocities \bar{u} and \bar{v} according to

$$(2.23) \quad \bar{u} = \frac{u}{U}$$

$$(2.24) \quad \bar{v} = \frac{v}{V} = \frac{1}{\epsilon} \frac{v}{U}$$

with

$$(2.25) \quad \epsilon = \frac{l}{\Lambda}.$$

- For the adimensionalization of convective terms, the reference for density is the density ρ_0 of the air at the usual conditions and reference for pressure is associated with the dynamic pressure $\rho_0 U^2$. We set

$$(2.26) \quad \bar{\rho} = \frac{\rho}{\rho_0}$$

$$(2.27) \quad \bar{p} = \frac{p}{\rho_0 U^2}.$$

The reference for internal energy is chosen in order to maintain the validity of the state equation (2.13) after adimensionalization. We set

$$(2.28) \quad \bar{e} = \frac{e}{U^2}$$

and we deduce from (2.13), (2.26) (2.27) and (2.28) the state equation between these new variables :

$$(2.29) \quad \bar{p} = (\gamma - 1) \bar{\rho} \bar{e}.$$

- The Reynolds number R_e appears from the dissipation terms in the momentum equations (2.15) and (2.16)

$$(2.30) \quad R_e = \frac{\rho_0 U \Lambda}{\mu},$$

the Prandtl number P_r is defined from the heat fluxes in the energy equation (2.17)

$$(2.31) \quad P_r = \frac{\mu C_p}{k}$$

and a reference scale for temperature is defined by $\frac{U^2}{C_p}$:

$$(2.32) \quad \bar{T} = \frac{C_p T}{U^2}.$$

The Joule-Gay Lussac law for polytropic gas can be rewritten in terms of dimensionless energy \bar{e} and temperature \bar{T} according to

$$(2.33) \quad \bar{e} = \gamma \bar{T}.$$

- Then the adimensionalized Navier Stokes equations take the following form

$$(2.34) \quad \frac{\partial \bar{\rho}}{\partial \bar{t}} + \frac{\partial}{\partial \bar{x}} (\bar{\rho} \bar{u}) + \frac{\partial}{\partial \bar{y}} (\bar{\rho} \bar{v}) = 0$$

$$(2.35) \quad \left\{ \begin{aligned} \frac{\partial}{\partial \bar{t}}(\bar{\rho}\bar{u}) + \frac{\partial}{\partial \bar{x}}(\bar{\rho}\bar{u}^2 + \bar{p}) + \frac{\partial}{\partial \bar{y}}(\bar{\rho}\bar{u}\bar{v}) &= \\ &= \frac{1}{R_e} \left[\frac{\partial}{\partial \bar{x}} \left(\frac{4}{3} \frac{\partial \bar{u}}{\partial \bar{x}} + \frac{1}{3} \frac{\partial \bar{v}}{\partial \bar{y}} \right) + \frac{1}{\epsilon^2} \frac{\partial^2 \bar{u}}{\partial \bar{y}^2} \right] \end{aligned} \right.$$

$$(2.36) \quad \left\{ \begin{aligned} \frac{\partial}{\partial \bar{t}}(\bar{\rho}\bar{v}) + \frac{\partial}{\partial \bar{x}}(\bar{\rho}\bar{u}\bar{v}) + \frac{\partial}{\partial \bar{y}}(\bar{\rho}\bar{v}^2 + \frac{1}{\epsilon^2}\bar{p}) &= \\ &= \frac{1}{R_e} \left[\frac{\partial^2 \bar{v}}{\partial \bar{x}^2} + \frac{1}{\epsilon^2} \frac{\partial}{\partial \bar{y}} \left(\frac{1}{3} \frac{\partial \bar{u}}{\partial \bar{x}} + \frac{4}{3} \frac{\partial \bar{v}}{\partial \bar{y}} \right) \right] \end{aligned} \right.$$

$$(2.37) \quad \left\{ \begin{aligned} &\frac{\partial}{\partial \bar{t}} \left(\bar{\rho} \left(\bar{e} + \frac{1}{2}(\bar{u}^2 + \epsilon^2\bar{v}^2) \right) \right) + \\ &+ \frac{\partial}{\partial \bar{x}} \left(\bar{\rho}\bar{u} \left(\bar{e} + \frac{1}{2}(\bar{u}^2 + \epsilon^2\bar{v}^2) \right) + \bar{p}\bar{u} \right) + \\ &+ \frac{\partial}{\partial \bar{y}} \left(\bar{\rho}\bar{v} \left(\bar{e} + \frac{1}{2}(\bar{u}^2 + \epsilon^2\bar{v}^2) \right) + \bar{p}\bar{v} \right) = \\ &= \frac{1}{R_e} \frac{\partial}{\partial \bar{x}} \left[\bar{u} \left(\frac{4}{3} \frac{\partial \bar{u}}{\partial \bar{x}} - \frac{2}{3} \frac{\partial \bar{v}}{\partial \bar{y}} \right) + \bar{v} \left(\frac{\partial \bar{u}}{\partial \bar{y}} + \epsilon^2 \frac{\partial \bar{v}}{\partial \bar{x}} \right) \right] + \\ &+ \frac{1}{R_e} \frac{\partial}{\partial \bar{y}} \left[\bar{u} \left(\frac{\partial \bar{v}}{\partial \bar{x}} + \frac{1}{\epsilon^2} \frac{\partial \bar{u}}{\partial \bar{y}} \right) + \bar{v} \left(\frac{4}{3} \frac{\partial \bar{v}}{\partial \bar{y}} - \frac{2}{3} \frac{\partial \bar{u}}{\partial \bar{x}} \right) \right] + \\ &+ \frac{1}{R_e} \frac{1}{P_r} \left(\frac{\partial^2 \bar{T}}{\partial \bar{x}^2} + \frac{1}{\epsilon^2} \frac{\partial^2 \bar{T}}{\partial \bar{y}^2} \right). \end{aligned} \right.$$

- The boundary conditions associated with these equations are of Dirichlet type on the boundary of the pipe :

$$(2.38) \quad \bar{u}(x, y = -h) = \bar{u}(x, y = h) = 0$$

$$(2.39) \quad \bar{v}(x, y = -h) = \bar{v}(x, y = h) = 0$$

$$(2.40) \quad \bar{T}(x, y = -h) = \bar{T}(x, y = h) = \bar{T}_0$$

where \bar{T}_0 is the nondimensionless temperature given at the boundary of the pipe.

- We observe first that the velocities \bar{u} and \bar{v} have the same order of magnitude and in consequence, due to the fact that

$$(2.41) \quad \epsilon^2 \ll 1$$

we can neglect in the left hand side of equation (2.37) the \bar{v} term compared to the \bar{u} term.

- We make the hypothesis that a typical distance for longitudinal variation of physical fields is of the order Λ . In particular $\frac{\partial u}{\partial x} \simeq \frac{U}{\Lambda}$ and in consequence

$$(2.42) \quad \frac{\partial \bar{u}}{\partial \bar{x}} \simeq 1.$$

We observe that no bigger gradients than $\frac{1}{\Lambda}$ are taken in consideration into hypothesis (2.42) which means that the flow is regular and that no turbulence occurs. In an analogous way, a typical distance for transversal variation of all the fields is of the order of l and in particular $\frac{\partial v}{\partial y} \simeq \frac{V}{l} = \frac{U}{\Lambda}$ and we have again

$$(2.43) \quad \frac{\partial \bar{v}}{\partial \bar{y}} \simeq 1.$$

More generally all the differential expressions of the type $\frac{\partial^k \bar{w}}{\partial \bar{z}^k}$ with w equal to one of the physical fields ρ, u, v, T, e , variable z equal to t, x , or y and $k = 1, 2$, is finally of the order of 1 (see *e.g.* Schlichting [Sc55] or Cousteix [Co88]) :

$$(2.44) \quad \frac{\partial^k \bar{w}}{\partial \bar{z}^k} \simeq 1.$$

• When we sum linear combinations of such expressions with coefficients of the type 1 or $\frac{1}{\epsilon^2}$ (as in the right hand side of relation (2.35)), the leading term is the one that has the dominant factor $\frac{1}{\epsilon^2}$ as a coefficient. We neglect in the following all the other terms. After these approximations, we have derived the so-called Thin Layer Navier Stokes equations (see *e.g.* Baldwin-Lomax [BL78], Kutler-Chakravarthy-Lombard [KCL78] or Rubin and Tannehill [RT92]). We re-write them without any adimensionalization :

$$(2.45) \quad \frac{\partial \rho}{\partial t} + \frac{\partial}{\partial x}(\rho u) + \frac{\partial}{\partial y}(\rho v) = 0$$

$$(2.46) \quad \frac{\partial}{\partial t}(\rho u) + \frac{\partial}{\partial x}(\rho u^2 + p) + \frac{\partial}{\partial y}(\rho u v) = \mu \frac{\partial^2 u}{\partial y^2}$$

$$(2.47) \quad \frac{\partial p}{\partial y} = \mu \frac{\partial}{\partial y} \left(\frac{1}{3} \frac{\partial u}{\partial x} + \frac{4}{3} \frac{\partial v}{\partial y} \right)$$

$$(2.48) \quad \left\{ \begin{array}{l} \frac{\partial}{\partial t} \left(\rho \left(e + \frac{1}{2} u^2 \right) \right) + \frac{\partial}{\partial x} \left(\rho u \left(e + \frac{1}{2} u^2 \right) + p u \right) + \\ \quad + \frac{\partial}{\partial y} \left(\rho v \left(e + \frac{1}{2} u^2 \right) + p v \right) = \mu \frac{\partial}{\partial y} \left(u \frac{\partial u}{\partial y} \right) + k \frac{\partial^2 T}{\partial y^2}. \end{array} \right.$$

3) Perfect fluid for main flow.

• We suppose now that the flow in the pipe satisfies the thin layer Navier-Stokes equations (2.45)-(2.48) and for fixed time t and abscissa x , we integrate equation (2.45) between $y = -h$ and $y = +h$. We obtain in this way

$$(3.1) \quad \left\{ \begin{aligned} \frac{\partial}{\partial t} \left(\frac{1}{2h} \int_{-h}^h \rho(t, x, y) dy \right) + \frac{\partial}{\partial x} \left(\frac{1}{2h} \int_{-h}^h (\rho u)(t, x, y) dy \right) + \\ + \frac{1}{2h} \left((\rho v)(t, x, h) - (\rho v)(t, x, -h) \right) = 0. \end{aligned} \right.$$

Due to boundary condition (2.39), the third term in (3.1) is null. We introduce now the mean values of density, momentum and energy in each x section according to :

$$(3.2) \quad \tilde{\rho}(t, x) = \frac{1}{2h} \int_{-h}^h \rho(t, x, y) dy$$

$$(3.3) \quad \tilde{\rho}(t, x) \tilde{u}(t, x) = \frac{1}{2h} \int_{-h}^h (\rho u)(t, x, y) dy$$

$$(3.4) \quad \tilde{\rho}(t, x) \tilde{e}(t, x) + \frac{1}{2} \tilde{\rho}(t, x) \tilde{u}^2(t, x) = \frac{1}{2h} \int_{-h}^h \left(\rho e + \frac{1}{2} \rho u^2 \right)(t, x, y) dy.$$

In terms of these new variables, the conservation of mass stands as :

$$(3.5) \quad \frac{\partial \tilde{\rho}}{\partial t} + \frac{\partial}{\partial x} (\tilde{\rho} \tilde{u}) = 0.$$

• In a similar way we integrate the impulse and the energy equations in the thickness of the pipe. We get

$$(3.6) \quad \left\{ \begin{aligned} \frac{\partial}{\partial t} (\tilde{\rho} \tilde{u}) + \frac{\partial}{\partial x} \left(\frac{1}{2h} \int_{-h}^h (\rho u^2 + p)(t, x, y) dy \right) = \\ = \frac{\mu}{2h} \left(\frac{\partial u}{\partial y}(t, x, h) - \frac{\partial u}{\partial y}(t, x, -h) \right) \end{aligned} \right.$$

$$(3.7) \quad \left\{ \begin{aligned} \frac{\partial}{\partial t} \left(\tilde{\rho} \tilde{e} + \frac{1}{2} \tilde{\rho} \tilde{u}^2 \right) + \frac{\partial}{\partial x} \left(\frac{1}{2h} \int_{-h}^h \left(\rho u \left(e + \frac{u^2}{2} \right) + p u \right)(t, x, y) dy \right) = \\ = \frac{k}{2h} \left(\frac{\partial T}{\partial y}(t, x, h) - \frac{\partial T}{\partial y}(t, x, -h) \right) \end{aligned} \right.$$

due to boundary conditions (2.38) and (2.39).

• We make first the hypothesis that the fields are quasi-constant in each section of the pipe and second that they have a rapid variation in a boundary layer region of thickness δ , with the condition

$$(3.8) \quad S_h \equiv \frac{\delta}{h} \ll 1.$$

The first hypothesis is absolutely non trivial.

- In aerodynamics, it conducts (see *e.g.* Whitham [Wh74] and Msallam [Ms98]) to the shallow water equations when the following physical hypothesis is satisfied :

$$(3.9) \quad \frac{1}{R_e^{\text{aero}}} \frac{1}{S_h} \approx \frac{\delta}{L} \frac{h}{L} = \epsilon \frac{h}{L} \ll 1$$

due to hypothesis (2.1) and choice of variable ϵ done in (2.5).

- In acoustics, the Reynolds number is modified according to relation (2.9), *i.e.*

$$(3.10) \quad R_e^{\text{acou}} = \frac{\rho_0 c_0 \lambda}{2 \pi \mu}$$

and the hypothesis of quasi-constancy of all the fields in the main flow is satisfied under the hypothesis (Kergomard [Ke81], Menguy and Gilbert [MG97])

$$(3.11) \quad \frac{1}{R_e^{\text{acou}}} \frac{1}{S_h} \ll 1.$$

- This hypothesis can be justified as follow. Observe first that for a simple linear wave, the variation of pressure p_a due to acoustics satisfies the relation

$$(3.12) \quad p_a = \rho_0 c_0 u .$$

Second the transverse gradient of pressure $\frac{\partial p}{\partial y}$ satisfies at the first order a linearized version of equation (2.36) :

$$(3.13) \quad \left| \frac{\partial p}{\partial y} \right| = \left| \rho_0 \frac{\partial v}{\partial t} \right|$$

and the right hand side of this equation (3.13) can be evaluated as follow :

$$(3.14) \quad \frac{\partial p}{\partial y} \approx \rho_0 \frac{\delta}{\lambda} u \frac{1}{\tau} = \rho_0 u c_0 \left(\frac{\delta}{\lambda} \right)^2 \frac{1}{\delta}$$

because $\tau = \frac{\lambda}{c_0}$ where the thickness of the boundary layer δ is (see *e.g.* Lighthill [Li78]) of the order of $\frac{\lambda}{\sqrt{R_e^{\text{acou}}}}$:

$$(3.15) \quad \bar{\delta} = \frac{\delta}{\lambda} \approx \frac{1}{\sqrt{R_e^{\text{acou}}}} .$$

We insert relations (3.8), (3.12) and (3.15) inside (3.14) and obtain

$$(3.16) \quad \frac{\partial p}{\partial y} \approx \frac{p_a}{h} \frac{1}{R_e^{\text{acou}}} \frac{1}{S_h}.$$

The transverse variations of pressure are of the order of the axial variations of pressure multiplied by the factor $\frac{1}{R_e^{\text{acou}} S_h}$. Then relation (3.11) express that the transverse variation of pressure can be neglected compared with the axial ones.

- We observe also that

$$(3.17) \quad \frac{1}{R_e^{\text{acou}}} \frac{1}{S_h} = \left(\frac{\delta}{\lambda}\right)^2 \frac{h}{\delta} = \frac{\delta h}{\lambda^2} = \frac{\delta}{\lambda} \frac{h}{\lambda} \leq \frac{1}{4} \frac{1}{\sqrt{R_e^{\text{acou}}}} \ll 1$$

due to hypotheses (2.6), (3.8) and (3.15). Then hypothesis (3.11) is established even if the boundary layer thickness δ is greater than the order of magnitude of the characteristic length l of visco-thermic effects. Physically, it corresponds to neglect volume losses compared to wall losses.

- Under the hypothesis that all the fields are constant in the section

$$-(h - \delta) \leq y \leq (h - \delta),$$

we first observe that pressure \tilde{p} associated via the state equation (2.13) to mean density $\tilde{\rho}$ and mean internal energy \tilde{e} can be well approached by the mean value of pressure :

$$(3.18) \quad (\gamma - 1) \tilde{\rho} \tilde{e} \simeq \frac{1}{2h} \int_{-h}^h p(t, x, y) dy$$

as mentioned previously. In an analogous way, we have

$$(3.19) \quad \tilde{\rho} \tilde{u}^2 \simeq \frac{1}{2h} \int_{-h}^h (\rho u^2)(t, x, y) dy$$

$$(3.20) \quad \tilde{\rho} \tilde{u} \left(\tilde{e} + \frac{1}{2} \tilde{u}^2 \right) + \tilde{p} \tilde{u} \simeq \frac{1}{2h} \int_{-h}^h \left(\rho u \left(e + \frac{u^2}{2} \right) + pu \right) (t, x, y) dy.$$

All the hypotheses (3.18)-(3.20) suppose finally that mean values of a nonlinear function is quasi-equal to the same nonlinear function of the mean values. This hypothesis is correct when the nonlinear function is well approximated by a constant.

- We can now insert relations (3.18) to (3.20) inside equations (3.6) and (3.7). We obtain the final model for unidimensional perfect flow :

$$(3.21) \quad \tilde{p}(t, x) \equiv (\gamma - 1) \tilde{\rho} \tilde{e}$$

$$(3.22) \quad \frac{\partial \tilde{\rho}}{\partial t} + \frac{\partial}{\partial x} (\tilde{\rho} \tilde{u}) = 0.$$

$$(3.23) \quad \frac{\partial}{\partial t}(\tilde{\rho}\tilde{u}) + \frac{\partial}{\partial x}\left(\tilde{\rho}\tilde{u}^2 + \tilde{p}\right) = \frac{\mu}{2h} \left(\frac{\partial u}{\partial y}(t, x, h) - \frac{\partial u}{\partial y}(t, x, -h) \right)$$

$$(3.24) \quad \begin{cases} \frac{\partial}{\partial t}(\tilde{\rho}\tilde{e} + \frac{1}{2}\tilde{\rho}\tilde{u}^2) + \frac{\partial}{\partial x}\left(\tilde{\rho}\tilde{u}(\tilde{e} + \frac{1}{2}\tilde{u}^2) + \tilde{p}\tilde{u}\right) = \\ = \frac{k}{2h} \left(\frac{\partial T}{\partial y}(t, x, h) - \frac{\partial T}{\partial y}(t, x, -h) \right). \end{cases}$$

4) Acoustic boundary layer.

• We suppose as previously that the flow in the pipe satisfies the Thin Layer Navier Stokes equations (2.45)-(2.48). In the following, we look for the boundary layer ($y \leq -h + \delta$ or $y \geq h - \delta$). The previous Thin Layer Navier Stokes equations simplify and we obtain the equations of acoustic boundary layer [Ch64].

• First we suppose that some reference state with null velocity is given. It is a priori the air at usual atmospheric pressure p_0 and usual temperature θ_0 ; with the state law of perfect gas, the reference density ρ_0 is given. Second we search a field $\rho(t, x, y)$, $u(t, x, y)$, $T(t, x, y)$, $p(t, x, y)$ of the form

$$(4.1) \quad \begin{cases} \rho(t, x, y) = \rho_0 + \rho'(t, x, y) \\ u(t, x, y) = 0 + u'(t, x, y) \\ T(t, x, y) = \theta_0 + T'(t, x, y) \\ p(t, x, y) = p_0 + p'(t, x, y). \end{cases}$$

We linearize the equations (2.45)-(2.48) around the reference state (ρ_0, p_0, θ_0) . We suppose that we can neglect the nonlinear contributions of the boundary layer for studying the equations (3.21)-(3.24) of the main flow. We recall that these equations have been obtained by integrating the Thin Layer Navier Stokes equations on the complete width of the channel and the detailed analysis of the different contributions have been derived by Msallam [Ms98]. Recall that by doing this linear approximation, we neglect the acoustic streaming effect (see *e.g.* Batchelor [Ba67], Makarov and Ochmann [Mo97]), all separation effects inside the boundary layer (Merkli and Thoman [MT75]) and all random unstationary effects of turbulence [MT75]. The algebra is classical (Chester [Ch64]) and straightforward. We obtain

$$(4.2) \quad \frac{p'}{p_0} = \frac{\rho'}{\rho_0} + \frac{T'}{\theta_0}$$

$$(4.3) \quad \frac{\partial \rho'}{\partial t} + \rho_0 \operatorname{div} u' = 0.$$

$$(4.4) \quad \rho_0 \frac{\partial u'}{\partial t} - \mu \frac{\partial^2 u'}{\partial y^2} = - \frac{\partial p'}{\partial x}$$

$$(4.5) \quad \rho_0 C_p \frac{\partial T'}{\partial t} - k \frac{\partial^2 T'}{\partial y^2} = \frac{\partial p'}{\partial t}.$$

We note (with Chester [Ch64]) that equations (4.4) and (4.5) are two heat equations coupled via the right hand sides.

- The boundary conditions associated to (say) the bottom of the boundary layer ($y = -h$) are :

$$(4.6) \quad u'(t, x, y = -h) = 0.$$

$$(4.7) \quad T'(t, x, y = -h) = 0.$$

At the top of the boundary layer ($y \approx -h + \delta$), we must match the boundary layer flow with the main flow :

$$(4.8) \quad u'(t, x, y \rightarrow -h + \delta) \rightarrow (\text{velocity in the main flow})(t, x)$$

$$(4.9) \quad T'(t, x, y \rightarrow -h + \delta) + \theta_0 \rightarrow (\text{temperature in the main flow})(t, x).$$

5) The coupled problem.

- We couple in this section the main flow in the pipe described in section 3 with the acoustic boundary layer presented in part 4. More precisely, the main flow is described by three unknown functions (density, velocity, internal energy) :

$$(5.1) \quad [0, +\infty[\times [0, L] \ni (t, x) \mapsto (\rho(t, x), u(t, x), e(t, x)) \in [0, +\infty[\times \mathbb{R} \times [0, +\infty[$$

which represent the mean value in the section of the pipe of each field (denoted with a tilda in section 3). In the boundary layer, we suppose that the faces $y = \pm h$ are composed by symmetric flows and we fix some transverse variable $\eta \in [0, +\infty[$.

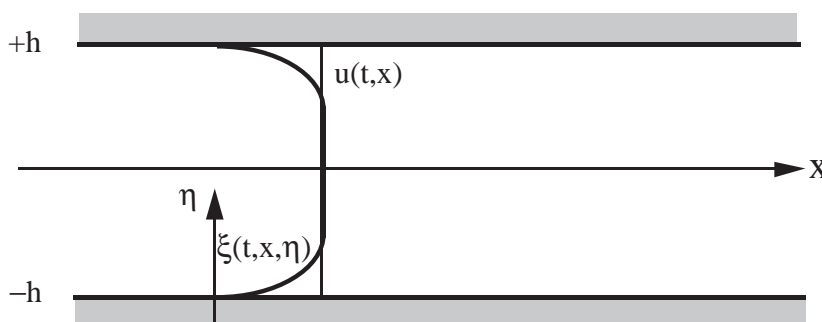


Figure 2 Velocity field $u(x, t)$ in the mean flow and velocity field $\xi(t, x, \eta)$ inside the boundary layer.

The unknowns are velocity ξ and temperature θ in the boundary layer :

$$(5.2) \quad [0, +\infty[\times [0, L] \times [0, +\infty[\ni (t, x, \eta) \mapsto (\xi(t, x, \eta), \theta(t, x, \eta)) \in \mathbb{R} \times [0, +\infty[$$

Notice the important point concerning the modelling : we consider on one hand **two** velocity fields u and ξ and on the other hand **two** temperature fields $T = e/C_v$ and θ .

- The transverse scale η for describing the boundary layer flow is very small compared to the transverse dimension h of the flow. Then it is consistent to set boundary conditions for $\eta \rightarrow +\infty$:

$$(5.3) \quad \begin{cases} \frac{\partial \xi}{\partial \eta}(t, x, \eta) \rightarrow 0 & \text{when } \eta \rightarrow +\infty \\ \frac{\partial \theta}{\partial \eta}(t, x, \eta) \rightarrow 0 & \text{when } \eta \rightarrow +\infty \end{cases}$$

and we have done this particular choice in our simulations. Nevertheless, stronger boundary conditions for $\eta \rightarrow +\infty$ that are compatible with the observed solutions in our numerical experiments could be the following ones :

$$(5.4) \quad \begin{cases} \xi(t, x, \eta) \rightarrow u(t, x) & \text{when } \eta \rightarrow +\infty \\ \theta(t, x, \eta) \rightarrow T(t, x) & \text{when } \eta \rightarrow +\infty. \end{cases}$$

- For $\eta = 0$, we just have to consider Dirichlet boundary conditions

$$(5.5) \quad \begin{cases} \xi(t, x, 0) = 0 \\ \theta(t, x, 0) = \theta_0 \end{cases}$$

where θ_0 is the value of imposed temperature on the walls.

- The partial differential equations for the evolution of main flow variables are simply derived from equations (3.21)-(3.24) ; the source terms of stress and thermal flux at the wall in the right hand side of equations (3.23) and (3.24) are nomore obtained by solving the Thin Layer Navier Stokes equations (2.45)-(2.48) but the ones coming from the boundary layer model (4.2)-(4.5). We obtain in this way :

$$(5.6) \quad p(t, x) \equiv (\gamma - 1) \rho e$$

$$(5.7) \quad \frac{\partial \rho}{\partial t} + \frac{\partial}{\partial x}(\rho u) = 0$$

$$(5.8) \quad \frac{\partial}{\partial t}(\rho u) + \frac{\partial}{\partial x}(\rho u^2 + p) = -\frac{\mu}{h} \frac{\partial \xi}{\partial \eta}(t, x, 0)$$

$$(5.9) \quad \frac{\partial}{\partial t}(\rho e + \frac{1}{2} \rho u^2) + \frac{\partial}{\partial x}(\rho u e + \frac{1}{2} \rho u^3 + p u) = -\frac{k}{h} \frac{\partial \theta}{\partial \eta}(t, x, 0).$$

- The evolution equations for boundary layer variables are obtained in a similar way from the heat equations (4.4)-(4.5) that model an acoustic boundary layer. With our coupled model, the pressure term comes from the main one-dimensional model and no more from the Thin Layer Navier Stokes equations ; it is therefore

considered as a source term and for this reason is placed on the right hand side of the equations. We get

$$(5.10) \quad \rho_0 \frac{\partial \xi}{\partial t} - \mu \frac{\partial^2 \xi}{\partial \eta^2} = - \frac{\partial p}{\partial x}$$

$$(5.11) \quad \rho_0 C_p \frac{\partial \theta}{\partial t} - k \frac{\partial^2 \theta}{\partial \eta^2} = \frac{\partial p}{\partial t}.$$

• We observe that equation (5.10) is a dynamic equation that allow the prediction of velocity field $\xi(t, x, \eta)$ as long as pressure field $p(t, x)$ is known. It is not so clear for temperature equation (5.11) for the variable θ due to the dynamic term $\frac{\partial p}{\partial t}$ on the right hand side. Nevertheless, following a remark of Brenier [Br97], system (5.5) (second equation) and (5.11) can be replaced by the new unknow function σ

$$(5.12) \quad \sigma = \rho_0 C_p \theta - p$$

that satisfies the following heat equation

$$(5.13) \quad \frac{\partial \sigma}{\partial t} - \frac{k}{\rho_0 C_p} \frac{\partial^2 \sigma}{\partial \eta^2} = 0$$

due to the fact that $\frac{\partial p}{\partial \eta} \equiv 0$. The following nonhomogeneous Dirichlet boundary condition is valid at the bottom of the boundary layer :

$$(5.14) \quad \sigma(t, x, 0) = \rho_0 C_p \theta_0 - p(t, x).$$

• It is clear that on one hand, that stress viscous term $\mu \frac{\partial \xi}{\partial \eta}(\eta = 0)$ and thermal flux $k \frac{\partial \theta}{\partial \eta}(\eta = 0)$ forces the main flow equations (5.7)-(5.9) and on the other hand that pressure field in the inviscid flow forces the boundary layer equations (5.10)-(5.11). We insist again on the fact that the main originality of our coupled model (5.6)-(5.11) consists of choosing **two** independent unknowns functions for velocity (in the main flow and in the bounday layer) and also **two** independent unknowns functions for temperature. We do not make the tentative to determine explicitly the boundary layer thickness $\delta(t, x)$ or the displacement thickness $\delta^*(t, x)$ (see *e.g.* Le Balleur [LB80]) in the way we set the coupled problem. In our approach, the boundary layer thickness for momentum and energy can be evaluated as a global (and nontrivial) result from the entire knowledge of functions $[0, +\infty[\ni \eta \mapsto \xi(t, x, \eta)$ and $[0, +\infty[\ni \eta \mapsto \theta(t, x, \eta)$.

• We recall briefly also the inflow-outflow boundary conditions at $x = 0$ and $x = L$ concerning the mean flow variables. At the inflow ($x = 0$), the flow is subsonic then two conditions have to be considered : for axample, we give on one hand some data concerning the input velocity field $u_0(t)$ or the input pressure

field $\pi_0(t)$ and on the other hand the fact that entropy is not dissipated at the entrance of the channel :

$$(5.15) \quad u(t, 0) = u_0(t) \quad \text{or} \quad p(t, 0) = \pi_0(t)$$

$$(5.16) \quad \frac{\partial}{\partial t} \left(\frac{p}{\rho^\gamma} \right) (t, 0) = 0.$$

At the outflow, the mean field remains subsonic and the theory of characteristics (see *e.g.* Kreiss [Kr70]) show that only one scalar boundary condition is sufficient to set correctly the problem ; we choice nonreflecting boundary conditions (see Whitham [Wh74] or Hedstrom [He79]) : the outgoing wave is a so-called C_+ simple wave [Wh74] *i.e.* both specific entropy $S \equiv \frac{p}{\rho^\gamma}$ and Riemann invariant

$R \equiv u - \frac{2c}{\gamma - 1}$ take constant values everywhere in this part of the flow. In consequence this Riemann invariant R is advected with all characteristic celerities without distorsion and in particular the one with $u - c$ velocity :

$$(5.17) \quad \left(\frac{\partial}{\partial t} \left(u - \frac{2c}{\gamma - 1} \right) + (u - c) \frac{\partial}{\partial x} \left(u - \frac{2c}{\gamma - 1} \right) \right) (t, L) = 0.$$

6) Generalization to axisymmetric geometry.

- In this section, the pipe is nomore a two-dimensional channel but a three-dimensional cylinder with an axisymmetric geometry. The length of the pipe is still denoted by L and the letter h is used for the radius instead of half of the section. Hypothesis (2.1) concerning ratio $\frac{h}{L}$ remains valid and we have

$$(6.1) \quad \frac{h}{L} \ll 1.$$

As is section 2, Thin Layer Navier Stokes equations are a good approximation of the flow inside the entire geometry and this model takes now the following algebraic form in this axisymmetric geometry :

$$(6.2) \quad \frac{\partial \rho}{\partial t} + \frac{\partial}{\partial x} (\rho u) + \frac{1}{y} \frac{\partial}{\partial y} (\rho v y) = 0$$

$$(6.3) \quad \frac{\partial}{\partial t} (\rho u) + \frac{\partial}{\partial x} (\rho u^2 + p) + \frac{1}{y} \frac{\partial}{\partial y} (\rho u v y) = \frac{\mu}{y} \frac{\partial}{\partial y} \left(y \frac{\partial u}{\partial y} \right)$$

$$(6.4) \quad \frac{1}{y} \frac{\partial}{\partial y} (\rho v^2 y + p y) = \frac{\mu}{y} \frac{\partial}{\partial y} \left(\frac{1}{3} \frac{\partial u}{\partial x} + \frac{4y}{3} \frac{\partial v}{\partial y} \right)$$

$$(6.5) \quad \begin{cases} \frac{\partial}{\partial t} \left(\rho \left(e + \frac{1}{2} u^2 \right) \right) + \frac{\partial}{\partial x} \left(\rho u \left(e + \frac{1}{2} u^2 \right) + p u \right) + \\ + \frac{1}{y} \frac{\partial}{\partial y} \left(\rho v y \left(e + \frac{1}{2} u^2 \right) + p v y \right) = \frac{\mu}{y} \frac{\partial}{\partial y} \left(u \frac{\partial u}{\partial y} \right) + \frac{k}{y} \frac{\partial}{\partial y} \left(y \frac{\partial T}{\partial y} \right) \end{cases}$$

$$(6.6) \quad 0 \leq y \leq h.$$

• The derivation of the coupled model can be conducted as in the previous sections. We first introduce the mean value of density, momentum and internal energy as in (3.2), (3.3) and (3.4) :

$$(6.7) \quad \tilde{\rho}(t, x) = \frac{2}{h^2} \int_0^h \rho(t, x, y) y \, dy$$

$$(6.8) \quad \tilde{\rho}(t, x) \tilde{u}(t, x) = \frac{2}{h^2} \int_0^h (\rho u)(t, x, y) y \, dy$$

$$(6.9) \quad \tilde{\rho}(t, x) \tilde{e}(t, x) + \frac{1}{2} \tilde{\rho}(t, x) \tilde{u}^2(t, x) = \frac{2}{h^2} \int_0^h \left(\rho e + \frac{1}{2} \rho u^2 \right)(t, x, y) y \, dy.$$

We multiply equation (6.2) by y , integrate between 0 and h and divide by $h^2 : 2$. We get

$$\frac{\partial \tilde{\rho}}{\partial t} + \frac{\partial}{\partial x} (\tilde{\rho} \tilde{u}) + \frac{2}{h^2} \left[\rho v y \right]_{y=0}^{y=h} = 0.$$

The term inside the brackets in the left hand side of the previous relation is null due to the no slip boundary condition :

$$(6.10) \quad u(t, x, h) = v(t, x, h) = 0,$$

and the conservation of mass becomes

$$(6.11) \quad \frac{\partial \tilde{\rho}}{\partial t} + \frac{\partial}{\partial x} (\tilde{\rho} \tilde{u}) = 0.$$

• We make the same operation for the momentum equation (6.3) :

$$(6.12) \quad \begin{cases} \frac{\partial}{\partial t} (\tilde{\rho} \tilde{u}) + \frac{\partial}{\partial x} \left(\frac{2}{h^2} \int_0^h (\rho u^2 + p)(t, x, y) y \, dy \right) + \\ + \frac{2}{h^2} \left[\rho y u v \right]_{y=0}^{y=h} = \frac{2\mu}{h^2} \left[y \frac{\partial u}{\partial y} \right]_{y=0}^{y=h} \end{cases}.$$

Under the same hypotheses concerning the boundary layer presented in section 3, we have :

$$(6.13) \quad (\gamma - 1) \tilde{\rho} \tilde{e} \simeq \frac{2}{h^2} \int_0^h p(t, x, y) y \, dy$$

$$(6.14) \quad \tilde{\rho} \tilde{u}^2 \simeq \frac{2}{h^2} \int_0^h (\rho u^2)(t, x, y) y \, dy.$$

We insert these evaluations inside relation (6.12) and obtain

$$(6.15) \quad \frac{\partial \tilde{\rho} \tilde{u}}{\partial t} + \frac{\partial}{\partial x} (\tilde{\rho} \tilde{u}^2 + \tilde{p}) = \frac{2\mu}{h} \left(\frac{\partial u}{\partial y} \right) (t, x, h)$$

with

$$(6.16) \quad \tilde{p}(t, x) \equiv (\gamma - 1) \tilde{\rho} \tilde{e}.$$

The treatment of the energy equation (6.5) is obtained by the same way, due to the boundary condition (6.10), approximations (6.13), (6.14) and

$$(6.17) \quad \tilde{\rho} \tilde{u} (\tilde{e} + \frac{1}{2} \tilde{u}^2) + \tilde{p} \tilde{u} \simeq \frac{2}{h^2} \int_0^h \left(\rho u \left(e + \frac{u^2}{2} \right) + pu \right) (t, x, y) y \, dy$$

$$(6.18) \quad \frac{\partial}{\partial t} (\tilde{\rho} \tilde{e} + \frac{1}{2} \tilde{\rho} \tilde{u}^2) + \frac{\partial}{\partial x} \left(\tilde{\rho} \tilde{u} (\tilde{e} + \frac{1}{2} \tilde{u}^2) + \tilde{p} \tilde{u} \right) = \frac{2k}{h} \frac{\partial T}{\partial y} (t, x, h).$$

- We change the notations, replace the "tilde" unknown functions by letters without tilda, denote by $\xi(t, x, \eta)$ the velocity in the boundary layer ($0 \leq \eta < +\infty$) and by $\theta(t, x, \eta)$ the temperature in the same conditions. Due to the relation

$$(6.19) \quad y = h - \eta, \quad \eta \approx 0$$

we have to change the sign in the right hand side of equations (6.15) and (6.18). We get finally, as in (5.6)-(5.9) :

$$(6.20) \quad p(t, x) \equiv (\gamma - 1) \rho e$$

$$(6.21) \quad \frac{\partial \rho}{\partial t} + \frac{\partial}{\partial x} (\rho u) = 0$$

$$(6.22) \quad \frac{\partial}{\partial t} (\rho u) + \frac{\partial}{\partial x} (\rho u^2 + p) = -\frac{2\mu}{h} \frac{\partial \xi}{\partial \eta} (t, x, 0)$$

$$(6.23) \quad \frac{\partial}{\partial t} (\rho e + \frac{1}{2} \rho u^2) + \frac{\partial}{\partial x} (\rho u e + \frac{1}{2} \rho u^3 + pu) = -\frac{2k}{h} \frac{\partial \theta}{\partial \eta} (t, x, 0).$$

We remark that there is just a factor of 2 that makes different the set of equations (6.22) (6.23) from the set of relations (5.8) (5.9).

- Inside the boundary layer, section 4 can be applied in a straightforward manner. We denote by u' the (infinitesimal) velocity, by p' the difference between pressure field p and ambient pressure p_0 and by T' the difference $T - \theta_0$. We have, due to the relations (4.4) and (4.5) :

$$(6.24) \quad \rho_0 \frac{\partial u'}{\partial t} - \frac{\mu}{y} \frac{\partial}{\partial y} \left(y \frac{\partial u'}{\partial y} \right) = -\frac{\partial p'}{\partial x}$$

$$(6.25) \quad \rho_0 C_p \frac{\partial T'}{\partial t} - \frac{k}{y} \frac{\partial}{\partial y} \left(y \frac{\partial T'}{\partial y} \right) = \frac{\partial p'}{\partial t}.$$

In the boundary layer, we have $y \approx h$ and the curvature effects due to geometry are associated to the radius h and this distance is very big compared with the thickness δ of the boundary layer :

$$(6.26) \quad \delta \ll h.$$

To fix the ideas, velocity field u' can be expanded with an ansatz of the type

$$(6.27) \quad u' = U f\left(\frac{y}{\delta}\right)$$

where $f(\bullet)$ is a regular function satisfying the conditions

$$(6.28) \quad f'(0) \approx f''(0) \approx f(1) \approx O(1).$$

Then $\frac{1}{h} \frac{\partial u'}{\partial y} \approx \frac{U}{h} \frac{1}{\delta} f'(0)$, $\frac{\partial^2 u'}{\partial y^2} \approx \frac{U}{\delta} \frac{1}{\delta} f''(0)$ and due to the relation

(6.26), the term $\frac{1}{h} \frac{\partial u'}{\partial y}$ can be neglected in comparison with the second term $\frac{\partial^2 u'}{\partial y^2}$.

- Finally the equations in the boundary layer can be written as

$$(6.29) \quad \rho_0 \frac{\partial \xi}{\partial t} - \mu \frac{\partial^2 \xi}{\partial \eta^2} = - \frac{\partial p}{\partial x}$$

$$(6.30) \quad \rho_0 C_p \frac{\partial \theta}{\partial t} - k \frac{\partial^2 \theta}{\partial \eta^2} = \frac{\partial p}{\partial t}$$

as in the two dimensional case. The coupled problem in the axisymmetric case is composed by the set of equations (6.20)-(6.23) and (6.29)-(6.30).

7) Numerical approximation of the coupled problem.

- The coupled system defined in section 5 is composed by five partial differential equations (5.7)-(5.11), the state law of perfect gas (5.6), the boundary conditions (5.3)(5.4) at the top-bottom of the pipe and by the inflow-outflow boundary conditions (5.15)-(5.17). We discretize this system of equations in the following manner.

- First we introduce some integer J and an associated space step Δx :

$$(7.1) \quad \Delta x = \frac{L}{J}$$

and some time step Δt is chosen below. We define the discrete variables ρ_j, u_j, e_j for density, velocity and energy at discrete point $x_j = j \Delta x$ ($j = 0, 1, 2, \dots, J$) and at time $t^m = m \Delta t$:

$$(7.2) \quad \begin{cases} \rho_j^m \approx \rho(m \Delta t, j \Delta x) \\ u_j^m \approx u(m \Delta t, j \Delta x) \\ e_j^m \approx e(m \Delta t, j \Delta x) \end{cases}$$

and we suppose that state equation is satisfied at time step $m \Delta t$ and at vertex $x_j = j \Delta x$:

$$(7.3) \quad p_j^m = (\gamma - 1) \rho_j^m e_j^m, \quad 0 \leq j \leq J, \quad 0 \leq m \leq n.$$

- We introduce the conservative variables W for mean flow :

$$W = \left(\rho, \rho u, \rho \left(e + \frac{u^2}{2} \right) \right)^t,$$

the physical flux function $f(W)$:

$$(7.4) \quad f(W) = \left(\rho u, \rho u^2 + p, \rho u \left(e + \frac{u^2}{2} \right) + p u \right)^t$$

and the source term due to the boundary layer :

$$(7.5) \quad G(W) = - \left(0, \beta \mu \frac{\partial \xi}{\partial \eta}(t, x, 0), \beta k \frac{\partial \theta}{\partial \eta}(t, x, 0) \right)^t.$$

where the variable β is defined by the condition

$$(7.6) \quad \beta = \begin{cases} 1 & \text{in the plane case of relations (5.7)-(5.9)} \\ 2 & \text{in the axisymmetric case of relations (6.21)-(6.23)}. \end{cases}$$

Then the equations (5.7)-(5.9) and (6.21)-(6.23) can be written in a more compact form :

$$(7.7) \quad \frac{\partial W}{\partial t} + \frac{\partial}{\partial x} f(W) = G(W).$$

- Variables (7.2) (for $j = 1, 2, \dots, J - 1$) are advanced between times $t^n = n \Delta t$ and $t^{n+1} = (n + 1) \Delta t$ according to the Lax-Wendroff [LW60] numerical scheme. This scheme is founded on a second order Taylor expansion in time of the conserved variables :

$$(7.8) \quad W_j^{n+1} = W_j^n + \Delta t \left(\frac{\partial W}{\partial t} \right)_j^n + \frac{1}{2} \Delta t^2 \left(\frac{\partial^2 W}{\partial t^2} \right)_j^n$$

that is exact up to a third order term relatively to variable Δt which is omitted in the numerical scheme (7.8). The first derivative in time $\left(\frac{\partial W}{\partial t} \right)_j^n$ is directly

evaluated thanks to equation (7.7) :

$$\left(\frac{\partial W}{\partial t} \right)_j^n = \left(G(W) \right)_j^n - \left(\frac{\partial f(W)}{\partial x} \right)_j^n$$

and more precisely

$$(7.9) \quad \left(\frac{\partial W}{\partial t} \right)_j^n = \begin{cases} \left(0, \beta\mu \frac{\partial \xi}{\partial \eta}(t^n, j \Delta x, 0), \beta k \frac{\partial \theta}{\partial \eta}(t^n, j \Delta x, 0) \right)^t \\ - \frac{1}{2 \Delta x} \left(\left[\left(\rho u, \rho u^2 + p, \rho u \left(e + \frac{u^2}{2} \right) + pu \right)^t \right]_{j+1}^n \right. \\ \left. - \left[\left(\rho u, \rho u^2 + p, \rho u \left(e + \frac{u^2}{2} \right) + pu \right)^t \right]_{j-1}^n \right). \end{cases}$$

The second derivative in time $\left(\frac{\partial^2 W}{\partial t^2} \right)_j^n$ is obtained by a derivation of equation (7.7) that takes into account the Schwarz property for partial derivatives :

$$\left(\frac{\partial^2 W}{\partial t^2} \right)_j^n = \left(\partial_t G(W) \right)_j^n - \left[\frac{\partial}{\partial x} \left(\frac{\partial f(W)}{\partial t} \right) \right]_j^n$$

and after discretization of the $\frac{\partial}{\partial x}$ operator by finite differences, we get :

$$(7.10) \quad \left(\frac{\partial^2 W}{\partial t^2} \right)_j^n = \begin{cases} \left(\partial_t G(W) \right)_j^n - \frac{1}{\Delta x} \left\{ \left(\partial_W f(W) \right)_{j+1/2}^n \bullet \left(\partial_t W \right)_{j+1/2}^n \right. \\ \left. - \left(\partial_W f(W) \right)_{j-1/2}^n \bullet \left(\partial_t W \right)_{j-1/2}^n \right\}. \end{cases}$$

We use classical expressions for the discrete operators presented in equation (7.10) : the time derivative of right hand side of equation (7.7) is local in space and will be evaluated “more above” :

$$(7.11) \quad \left(\partial_t G(W) \right)_j^n = \left[-\frac{\partial}{\partial t} \left(0, \beta\mu \frac{\partial \xi}{\partial \eta}(t^n, j \Delta x, 0), \beta k \frac{\partial \theta}{\partial \eta}(t^n, j \Delta x, 0) \right)^t \right]_j^n,$$

the jacobian matrix $\left(\partial_W f(W) \right)_{j+1/2}^n$ at the intermediate point $(j+1/2)\Delta x$ is evaluated thanks to a simple two-point mean value formula :

$$(7.12) \quad \left(\partial_W f(W) \right)_{j+1/2}^n = \begin{cases} \frac{1}{2} \left\{ \left[\frac{\partial \left(\rho u, \rho u^2 + p, \rho u \left(e + \frac{u^2}{2} \right) + pu \right)^t}{\partial \left(\rho, \rho u, \rho \left(e + \frac{u^2}{2} \right) \right)^t} \right]_j^n \right. \\ \left. + \left[\frac{\partial \left(\rho u, \rho u^2 + p, \rho u \left(e + \frac{u^2}{2} \right) + pu \right)^t}{\partial \left(\rho, \rho u, \rho \left(e + \frac{u^2}{2} \right) \right)^t} \right]_{j+1}^n \right\}, \end{cases}$$

and the time derivative of conservative variables at intermediate point $(j+1/2)\Delta x$ is obtained with a centered scheme :

$$(7.13) \quad (\partial_t W)_{j+1/2}^n = \begin{cases} \frac{1}{2} \left\{ \left(0, \beta \mu \frac{\partial \xi}{\partial \eta}(t^n, j \Delta x, 0), \beta k \frac{\partial \theta}{\partial \eta}(t^n, j \Delta x, 0) \right)^t + \right. \\ \left. \left(0, \beta \mu \frac{\partial \xi}{\partial \eta}(t^n, (j+1)\Delta x, 0), \beta k \frac{\partial \theta}{\partial \eta}(t^n, (j+1)\Delta x, 0) \right)^t \right\} \\ - \frac{1}{\Delta x} \left(\left[\left(\rho u, \rho u^2 + p, \rho u \left(e + \frac{u^2}{2} \right) + pu \right)^t \right]_{j+1}^n \right. \\ \left. - \left[\left(\rho u, \rho u^2 + p, \rho u \left(e + \frac{u^2}{2} \right) + pu \right)^t \right]_j^n \right). \end{cases}$$

- The source term $G(W)$ (relation (7.5)) is simple to represent with an integral formula, due to the simple structure of heat equations (5.10) and (5.11). We have (see *e.g.* Morse and Feshbach [MF53]) :

$$(7.14) \quad \operatorname{erf}(\chi) \equiv \frac{2}{\sqrt{\pi}} \int_0^\chi e^{-\sigma^2} d\sigma,$$

$$(7.15) \quad \xi(t, x, \eta) = -\frac{1}{\rho_0} \int_0^t \frac{\partial p}{\partial x}(z, x) \operatorname{erf} \left[\frac{\eta}{\sqrt{4 \frac{\mu}{\rho_0} (t-z)}} \right] dz$$

$$(7.16) \quad \theta(t, x, \eta) = \theta_0 + \frac{1}{\rho_0 C_p} \int_0^t \frac{\partial p}{\partial t}(z, x) \operatorname{erf} \left[\frac{\eta}{\sqrt{4 \frac{k}{\rho_0 C_p} (t-z)}} \right] dz,$$

and after derivation relatively to transverse variable η

$$(7.17) \quad \frac{\partial \xi}{\partial \eta}(t, x, 0) = -\frac{1}{\mu} \int_0^t \frac{\partial p}{\partial x}(t-z, x) \sqrt{\frac{\mu}{\rho_0 \pi z}} dz$$

$$(7.18) \quad \frac{\partial \theta}{\partial \eta}(t, x, 0) = \frac{1}{k} \int_0^t \frac{\partial p}{\partial t}(t-z, x) \sqrt{\frac{\mu}{\rho_0 C_p \pi z}} dz.$$

In consequence, the source term $(G(W))_j^n$ is numerically evaluated according to

$$(7.19) \quad (G(W))_j^n = \begin{pmatrix} 0 \\ \beta \sum_{m=0}^{n-1} \int_{m\Delta t}^{(m+1)\Delta t} \frac{\partial p}{\partial x}(n\Delta t - z, x_j) \sqrt{\frac{\mu}{\rho_0 \pi z}} dz \\ -\beta \sum_{m=0}^{n-1} \int_{m\Delta t}^{(m+1)\Delta t} \frac{\partial p}{\partial t}(n\Delta t - z, x_j) \sqrt{\frac{\mu}{\rho_0 C_p \pi z}} dz \end{pmatrix}.$$

The intermediate integrals in the second line of right hand side of (7.19) is approached with a two-point quadrature formula relatively to the measure $\frac{dz}{\sqrt{z}}$:

$$(7.20) \quad \int_a^b \varphi(z) \frac{dz}{\sqrt{z}} \approx \frac{1}{2} (\varphi(a) + \varphi(b)) \int_a^b \frac{dz}{\sqrt{z}} = (\varphi(a) + \varphi(b)) \frac{b-a}{\sqrt{a} + \sqrt{b}}$$

and integrals in third line of relation (7.19) are numerically approached by a one-point quadrature formula :

$$(7.21) \quad \int_a^b \varphi(z) \frac{dz}{\sqrt{z}} \approx \varphi\left(\frac{a+b}{2}\right) \int_a^b \frac{dz}{\sqrt{z}} = 2\varphi\left(\frac{a+b}{2}\right) \frac{b-a}{\sqrt{a} + \sqrt{b}}.$$

We deduce, due to quadrature relations (7.20)-(7.21) and elementary use of finite differences :

$$\begin{cases} \left(G_2(W)\right)_j^n = \\ = \beta \sum_{m=0}^{n-1} \frac{\sqrt{\Delta t}}{2\Delta x} \left[(p_{j+1}^{n-m-1} + p_{j+1}^{n-m}) - (p_{j-1}^{n-m-1} + p_{j-1}^{n-m}) \right] \sqrt{\frac{\mu}{\rho_0 \pi}} \frac{1}{\sqrt{m} + \sqrt{m+1}} \end{cases}$$

$$\left(G_3(W)\right)_j^n = -2\beta \sum_{m=0}^{n-1} \frac{1}{\sqrt{\Delta t}} \left[p_j^{n-m} - p_j^{n-m-1} \right] \sqrt{\frac{\mu}{\rho_0 C_p \pi}} \frac{1}{\sqrt{m} + \sqrt{m+1}}$$

and finally :

$$(7.22) \quad \left(G(W)\right)_j^n = \left(0, \left(G_2(W)\right)_j^n, \left(G_3(W)\right)_j^n \right)^t.$$

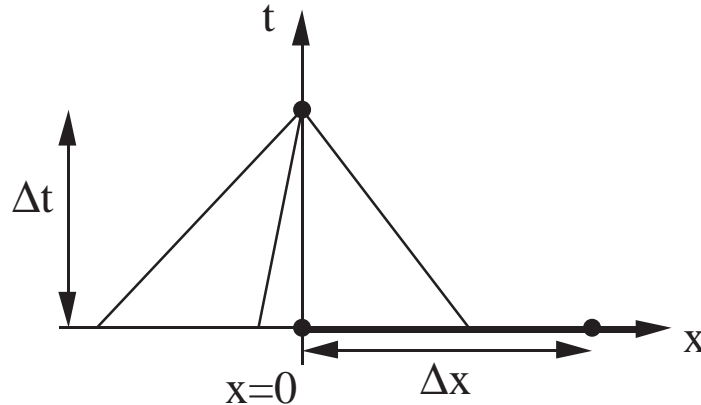


Figure 3 Characteristic directions at the entrance $x = 0$.

From previous evaluations, the time derivative of the source term $(\partial_t G(W))_j^n$ is computed with a simple first order scheme :

$$(7.23) \quad (\partial_t G(W))_j^n = \left(0, \frac{G_2(W)_j^n - G_2(W)_j^{n-1}}{\Delta t}, \frac{G_3(W)_j^n - G_3(W)_j^{n-1}}{\Delta t} \right).$$

• We neglect the boundary layers when considering numerically the boundary conditions at the input and at the output of the domain. The boundary conditions at $j = 0$ and $j = J$ are numerically implemented using the method of characteristics (see *e.g.* Whitham [Wh74]). We distinguish between three cases : input pressure wave, input simple velocity wave and nonreflecting output. In the case of an input pressure wave (at $j = 0$), two characteristics directions are going inside the computational domain (for celerities u and $u + c$) and one (associated with celerity $u - c$) is going outside (see Figure 3). We wish to define the state W_0^{n+1} at the first mesh point and at time $n + 1$; all the states at time level n are supposed to be given and the pressure field at time level $n + 1$ is imposed to be equal to some numerical value π^{n+1} due to the boundary condition. We denote by c_0 , p_0 and S_0 respectively the sound celerity, the pressure and the entropy of the air at rest at usual conditions of temperature and pressure. We first determine an external sound celerity c_e and an external velocity u_e associated with a C_+ input wave ; we have classically from locally linearized theory [Wh74] :

$$(7.24) \quad u_e = \frac{\pi^{n+1} - p_0}{\rho_0 c_0}$$

$$(7.25) \quad c_e = c_0 + \frac{\gamma - 1}{2} u_e.$$

Secondly we interpolate data at time level n and at the foot-point P going backward along the $u - c$ characteristics starting at t^{n+1} from $x = 0$:

$$(7.26) \quad W_P = \left(1 - \frac{u_0^n - c_0^n}{\Delta t} \right) W_0^n + \frac{u_0^n - c_0^n}{\Delta t} W_1^n.$$

The state W_0^{n+1} is finally defined by the following three conditions : the characteristic variable associated to the $u - c$ wave is constant between states W_P and W_0^{n+1} :

$$(7.27) \quad u_0^{n+1} - \frac{2c_0^{n+1}}{\gamma - 1} = u_P - \frac{2c_P}{\gamma - 1},$$

the entropy of state W_P is equal to the entropy at rest :

$$(7.28) \quad S_0^{n+1} = S_0$$

and the characteristic variable associated to the $u + c$ wave is constant between external state and state W_0^{n+1} :

$$(7.29) \quad u_0^{n+1} + \frac{2c_0^{n+1}}{\gamma - 1} = u_e + \frac{2c_e}{\gamma - 1}.$$

With this implementation, the single pressure datum variable π^{n+1} is used for two incoming waves and the outgoing wave is not reflected. We remark that, as in [DF89], nothing in what we have done imposes strongly the condition $p(W_0^{n+1}) = \pi^{n+1}$. In some sense, this boundary condition is transparent to the outgoing waves.

- We use the same notations for the input simple velocity wave associated to datum U^{n+1} at the time level under study. This datum is supposed to be sufficiently small in order to be considered as an acoustic velocity. We first determine the celerity of an external state W_e by a relation similar to (7.24) :

$$(7.30) \quad c_e = c_0 + \frac{\gamma - 1}{2} U^{n+1},$$

we interpolate a state W_P at the foot of the $u - c$ characteristic direction using relation (7.26) and the boundary state W_0^{n+1} is computed according to relations (7.27) along the outgoing characteristic, (7.28) along the u characteristic direction and the following relation along the $u + c$ incoming characteristic :

$$(7.31) \quad u_0^{n+1} + \frac{2c_0^{n+1}}{\gamma - 1} = U^{n+1} + \frac{2c_e}{\gamma - 1}.$$

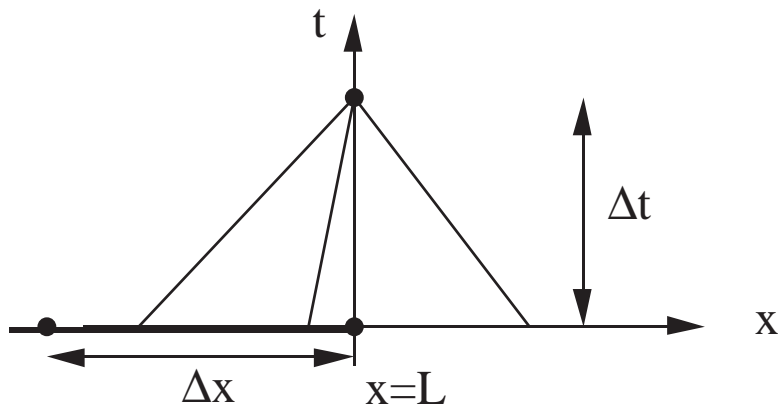


Figure 4 Nonreflecting output at $x = L$.

- For a nonreflecting output at $x = L$ and $j = J$ (see Figure 4), the external state is the air at rest and is obtained by going backward along the $u - c$ characteristic direction :

$$(7.32) \quad u_J^{n+1} - \frac{2c_J^{n+1}}{\gamma - 1} = -\frac{2c_0}{\gamma - 1}.$$

Concerning the waves going outside the computational domain, we define the foot-point Q associated with the $u + c$ characteristic direction with the same idea than previously :

$$(7.33) \quad W_Q = \left(1 - \frac{u_0^n + c_0^n}{\Delta t}\right) W_{J-1}^n + \frac{u_0^n + c_0^n}{\Delta t} W_J^n$$

and we say that the associated characteristic variable is constant between this state W_Q and state W_J^{n+1} :

$$(7.34) \quad u_J^{n+1} + \frac{2c_J^{n+1}}{\gamma - 1} = u_Q + \frac{2c_Q}{\gamma - 1}.$$

We suppose also than a relation similar to (7.28) determines the entropy at the limiting vertex :

$$(7.35) \quad S_J^{n+1} = S_0.$$

8) First test cases.

8.1) Nonlinear perfect oscillating fluid.

• In this sub-section, we neglect all the viscous effects. The continuous model is given by equations (5.6)-(5.9) with $\mu = 0$ and $k = 0$ and all the discrete equations correspond to Lax-Wendroff scheme (7.8)-(7.13) without source terms. The first test case consists of a simple wave going inside the domain $\{x \geq 0\}$. At time t equal to zero, the fluid is at rest (with pressure p_0 and temperature T_0 that correspond to usual thermodynamics conditions) and at $x = 0$, a source of velocity $u(0, t)$ is supposed to be given. It defines a simple wave, submitted to hypothesis

$$(8.1) \quad u - \frac{2c}{\gamma - 1} = -\frac{2c_0}{\gamma - 1}$$

and if $x = X(t)$ is the solution of the differential equation that defines the characteristic line, *i.e.*

$$(8.2) \quad \frac{dX}{dt} = u + c,$$

we have (see *e.g.* Whitham [Wh74])

$$(8.3) \quad u + \frac{2c}{\gamma - 1} = \text{Cste}.$$

By elimination of sound celerity c between equations (8.1) and (8.3), velocity $u(\bullet)$ has a constant value along the characteristic (8.2)-(8.3), and it is also the case for sound celerity. We deduce that $u + c$ depends only of its value for $x = 0$ and the slope of characteristic direction is constant :

$$(8.4) \quad u + c = c_0 + \frac{\gamma + 1}{2} u_0(t_0).$$

Then characteristic lines are straight lines. Moreover, if $x = L$ is some given abscissa, the time $t_L - t_0$ for the wave to propagate between $x = 0$ at time $t = t_0$ and $x = L$ at time $t = t_L$ is given according to the following relation :

$$(8.5) \quad t_L - t_0 = \frac{L}{u + c} = \frac{L}{c_0 + \frac{\gamma + 1}{2} u_0(t_0)} .$$

• We construct velocity field at the particular station $x = L$ with regular time steps τ . We search velocity $u(L, n\tau)$ according to the relation :

$$(8.6) \quad u(L, n\tau) = u_0(t_{0,n})$$

where $t_{0,n}$ is the solution of the following nonlinear equation :

$$(8.7) \quad n\tau - t_{0,n} = \frac{L}{c_0 + \frac{\gamma + 1}{2} u_0(t_{0,n})} .$$

Equation (8.7) is solved with the help of a Newton algorithm detailed in [Ms98] for a sinusoidal input velocity $u_0(\theta)$:

$$(8.8) \quad u_0(\theta) = U_0 \sin(\omega_0 \theta)$$

and the Newton algorithm is convergent without any problem as long as the characteristic lines does not intersect, *i.e.* under the condition

$$(8.9) \quad L < L_{\text{shock}} = \frac{2c_0^2}{(\gamma + 1)\omega_0 U_0} .$$

We introduce adimensionalized abscissa s relatively to L_{shock} :

$$(8.10) \quad s = \frac{x}{L_{\text{shock}}} .$$

The output velocity $u(L, \bullet)$ is a periodic function of time with period $T = 2\pi/\omega_0$ and parameter τ has been chosen such that

$$(8.11) \quad \tau = \frac{1}{2^N} \frac{2\pi}{\omega_0} \equiv \frac{1}{2^N} T_0$$

with a big integer N (of the order of 10 typically) in order to proceed a precise signal treatment. The nonlinear distorsion effect induces harmonics $k\omega_0$ ($k = 2, 3, \dots$) of fundamental pulsation ω_0 and they are predicted up to $k = 40$. Note that the time step τ for computing exact solution has been chosen sufficiently small in order to avoid aliasing effects when computing the fast Fourier transform.

MODEL FOR COUPLING A PERFECT FLOW WITH AN ACOUSTIC BOUNDARY LAYER

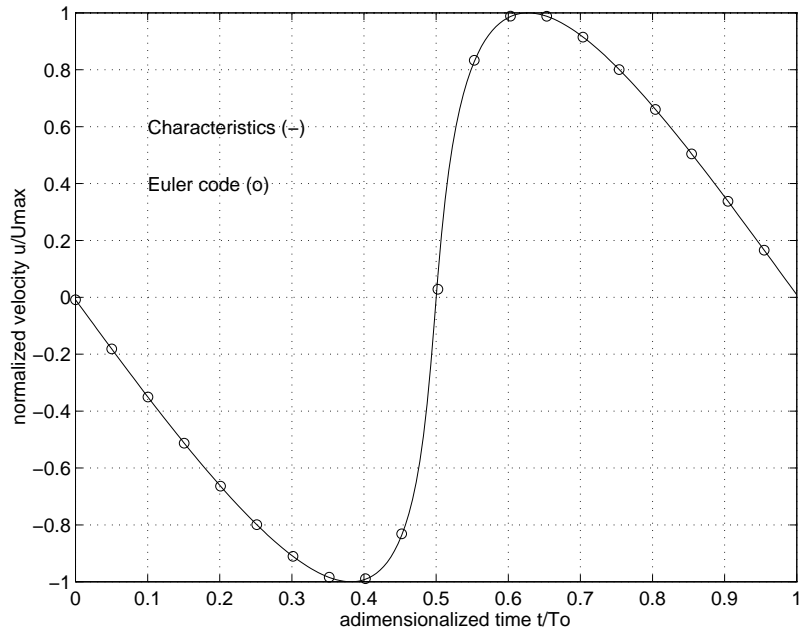


Figure 5 Signal at abscissa $s = 0.8$

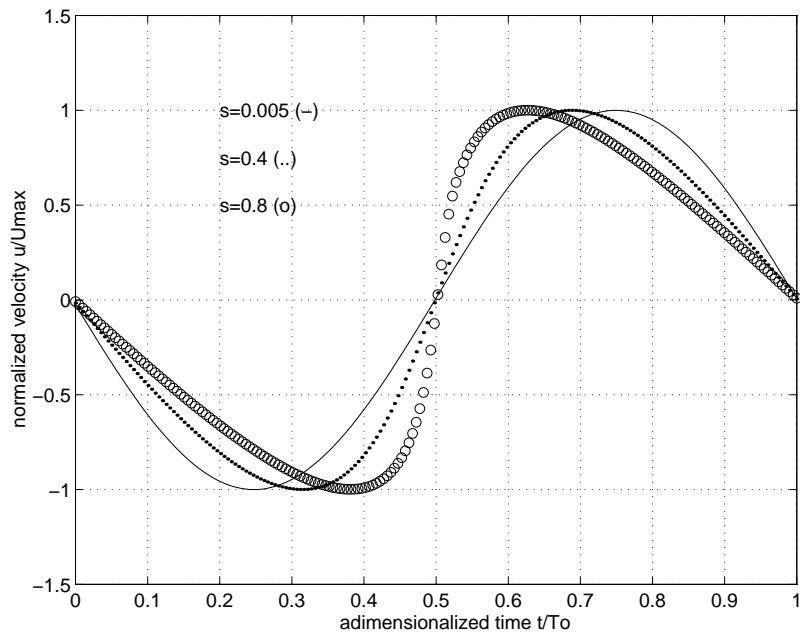


Figure 6 Signal for three abscissae

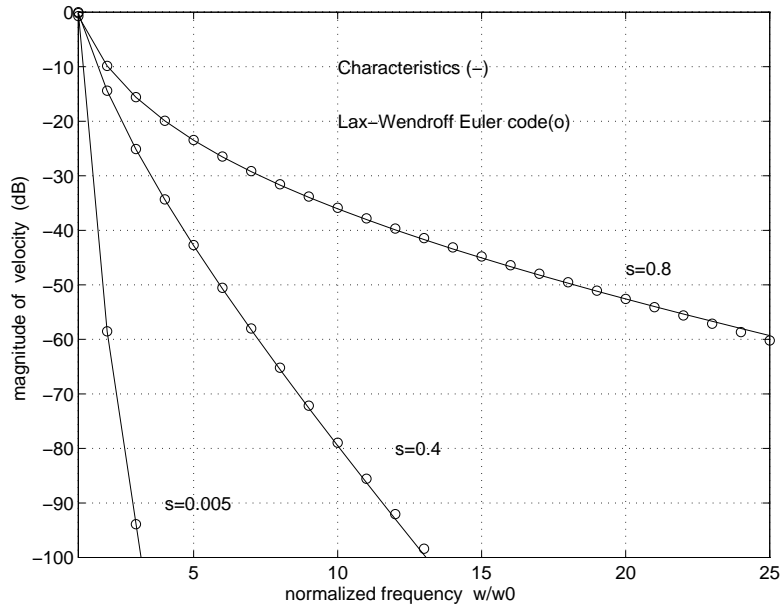


Figure 7 Magnitude spectrum for three abscissae

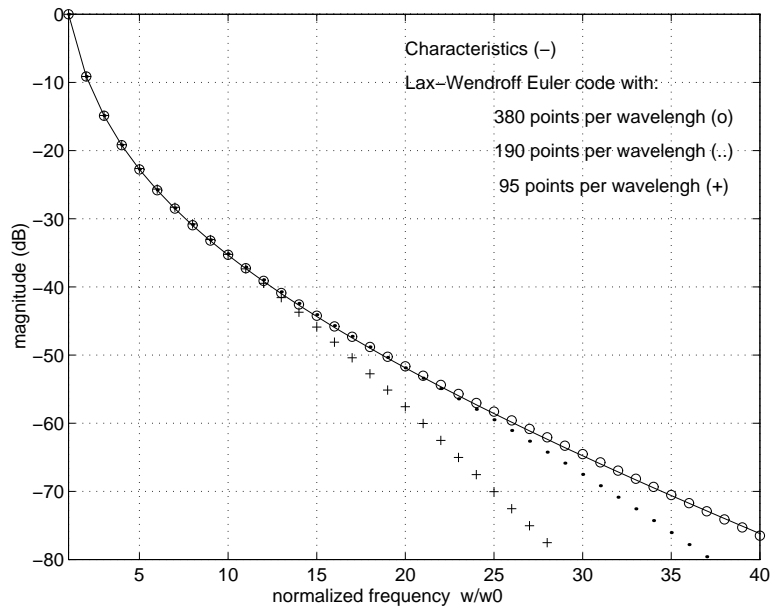


Figure 8 Influence of the space step Δx

- We first test the effect of non-absorbing boundary condition on the numerical flow computed with help of Lax-Wendroff scheme inside the domain. We consider two simulations on two computational domains with the same space step Δx . One domain is of length L and the other one is constructed in order to be sure that the boundary scheme is **not** active at $x = L$. Then we check that nonlinear

treatment (7.32)-(7.35) induces, for waves that compose the distorted signal at $x = L$, relative errors in velocity that are inferior to 2 % for waves containing more than 10 grid points.

- We compare this simple wave with the numerical solution computed with Lax-Wendroff scheme. We choose a simple sinusoidal velocity profile (8.8) at the inflow (see also (7.30) and (7.31) for the complementary boundary conditions at the inflow) and a non-reflecting boundary condition at $x = L$ (see also relations (7.31) to (7.35)). On Figure 5, we plot temporal output signal for exact (characteristics) and approached (Lax Wendroff) methods at station $s = 0.8$. We notice that Lax-Wendroff scheme is correct for prediction of this kind of nonlinear wave. We recover the distortion of the wave with a profile more and more sharp as variable s is increasing. We compare three results for the Lax Wendroff scheme at $s = 0.005, 0.4$ and 0.8 on Figure 6 and the associated spectra for these three locations on Figure 7. We verify on Figure 7 that distortion induces an enrichment of spectrum with a transfer of energy from low frequency to higher frequencies. Moreover, comparison of spectra for both methods shows that Lax-Wendroff scheme is operational for good prediction of output signal. We compare also spectra of output signals for different values of space steps Δx with constant CFL number that induces proportional values of Δt . For this particular simulation ($u_0(\bullet)$ given by relation (8.8) and $s = 0.8$) we observe (Figure 8) that numerical damping is compatible with harmonic $k = 15$ for 100 temporal points by period (*i.e.* $\frac{95}{15} \approx 6.3$ points for this particular harmonic) and with harmonic $k = 25$ for 190 points by time period ($\frac{190}{25} = 7.6$ points for one period).

8.2) Linear wave with visco-thermal boundary layer effects.

- In this sub-section, we compare our numerical model with the linear Kirchhoff theory obtained by linearizing convective effects around a null velocity. We refer to Bruneau et al [BHKP89] for this classical approach in the context of first order theory with thin boundary layer. Recall that a wave with pulsation ω can be a particular solution of linear Kirchhoff theory if the phase

$$(8.12) \quad \Phi = \omega t - K x$$

admits a dispersion relation of the type

$$(8.13) \quad K = \frac{\omega}{c'(\omega)} - i \alpha(\omega)$$

with

$$(8.14) \quad c'(\omega) = c_0 \left[1 - \left(\sqrt{\frac{\mu}{\rho_0 c_0}} + (\gamma - 1) \sqrt{\frac{k}{\rho_0 c_0 C_p}} \right) \frac{c_0}{2 h \omega} \right]$$

$$(8.15) \quad \alpha(\omega) = \left(\sqrt{\frac{\mu}{\rho_0 c_0}} + (\gamma - 1) \sqrt{\frac{k}{\rho_0 c_0 C_p}} \right) \frac{c_0}{2 h \omega}.$$

As long as the wave propagate, there is dispersion and damping of this wave. Dispersion is due to the fact that local phase velocity $c'(\omega)$ depends on frequency (see relation (8.14)). Damping is associated to the real part of the constant of propagation and $\alpha(\omega)$ is a damping coefficient.

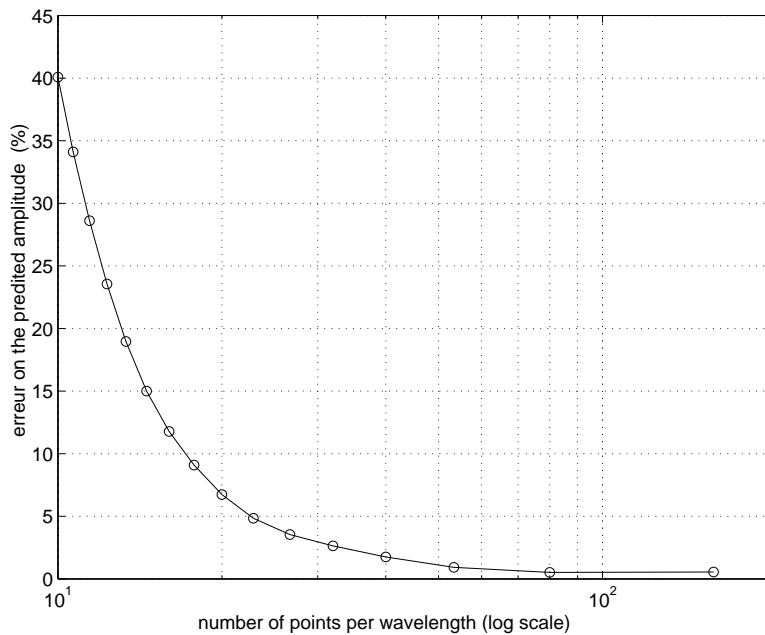


Figure 9 Relative error on amplitude between the Kirchhoff theory and the Lax-Wendroff code

- Sinusoidal wave of small amplitude have been simulated by the numerical model. In order to avoid the essential of nonlinear effects, a very small amplitude has been chosen for the wave. We simulate the propagation of an acoustic wave. The sinusoidal input profile is computed over a distance L physically of the order of 1 meter in a pipe of diameter of the order of 1 centimeter. We compare both amplitudes of the waves in the first case by using Kirchhoff model and in the second case with the pure numerical solver. The relative errors of the predicted amplitude are plotted on Figure 9. We use as space variable the number of grid points for one length wave. With more than 25 points by length wave, we observe that relative error for pressure field is inferior to 5%. The results concerning the phase obey to the same conclusion.

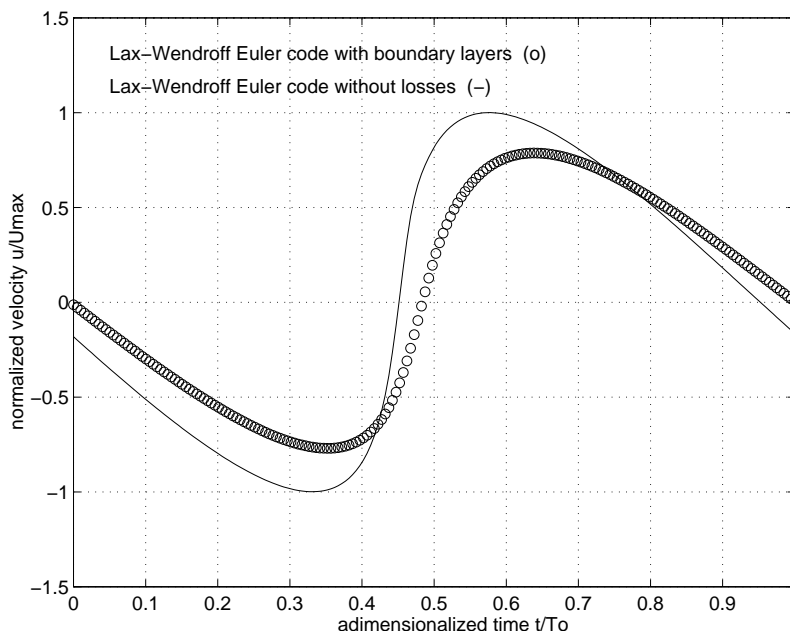


Figure 10 Comparison of flow field at $s = 0.8$ with and without losses

8.3) Combined nonlinear propagation and linear boundary layer.

- In this sub-section, we compare the shape of the wave with and without visco-thermal boundary layer. Observe that view results are available in the literature for this kind of elementary coupled problem. First comparison have been done with results obtained independently by Menguy and Gilbert [MG97b]. Figure 10 presents a temporal signal of velocity at fixed abscissa $s = 0.8$. There is an important damping of the wave and we recover that wavefront is less sharp with the presence of the boundary layer. Notice here the important remark that viscosity associated to the boundary layer is much more important that the one due to the thin layer Navier Stokes equations.

8.4) Trombone modelling.

- In [HGMW96], Hirschberg, Gilbert, Wijnands and the first author have demonstrated experimentally that for high level of amplitude (*forte*, *fortissimo*), there are important nonlinear propagation effects in the trombone which can lead to shock waves. From a modelling point of view, the slide of a trombone can be viewed in first approximation as unidimensional pipe of length of the order of 1.5 meter and radius $h = 7$ mm. A typical incident pressure wave at the entrance of the slide is propagating along the slide. It is a low frequency signal. At the output, we use an absorbing boundary condition. In fact, a complete model of trombone would include the discretization of the bell. But in the strong flaring part of the bell, the flow is no more quasi-unidimensional and our model is no more relevant (see Amir, Pagneux and Kergomard [APK97]). Because the slide is the

largest length with a cylindrical shape of the instrument, we conjecture that the essential of nonlinear effects occur in this part of the instrument. We restrict our simulations to the slide alone and make the hypothesis that nonlinear interaction between incident and reflected waves are negligible. This hypothesis has been verified with numerical tests [Ms98].

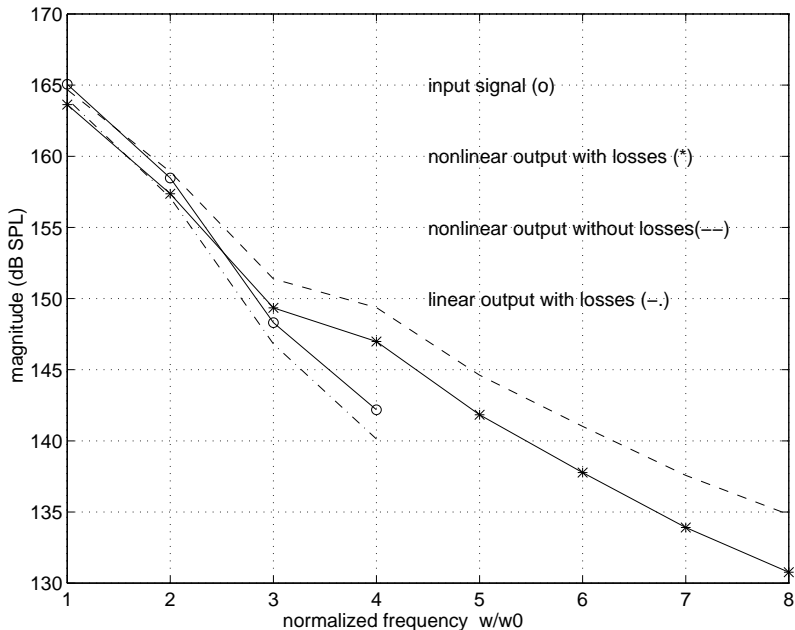


Figure 11 Magnitude spectrum at the output of the slide

- We have synthesised a typical input signal containing four harmonics. This signal has been propagated with a linear propagation with losses and with nonlinear advection with and without losses. Figure 11 represents these three output signals. There is of course no creation of superior harmonics with linear propagation (done with linearized computer software developed by Quinez [Qu95]). We recover the four initial input modes and damping is visible (2 dB) on the sound pressure level in Figure 11. With nonlinear propagation without losses, new harmonics for $k \geq 5$ are created. Moreover the amplitude of all the harmonics (except the first one) is amplified by nonlinear propagation. This corresponds to transfer of energy from lowest frequency to higher frequencies in order to go towards thermostatics equilibrium where we have equi-partition of the energy between all the modes. With both nonlinear and linear effects, previous results are damped with an amplitude varying between 1 and 5 dB for the 8 first modes. The effect of losses compensates the one of nonlinear propagation. Nevertheless, nonlinear effects dominate the dynamics. For example the amplitude of the 4th mode is increased of 5 dB compared to the input signal.

- Our numerical results confirm previous experiments done in Eindhoven : trombone's radiated sound is enriched by nonlinear effects which occurs in the instrument. This effect is known by the musicians as the "brassy" sound, typical for the trombone at loud tones (see *e.g.* [GM98]). Some sonor amplitude examples are available on the net at the following <http://www.icp.inpg.fr/~pelorson/sons.html>.

9) Conclusion, acknowledgments.

- In this study, we have proposed to use the Thin Layer Navier Stokes equations as primitive ones to study propagation effects in thin pipes. This complete model neglects diffusive effects in the stream direction. Second, we have derived from this primitive set of partial differential equations a coupled model of five equations that takes into account both nonlinear uni-dimensional propagation and linear diffusion in acoustic linear boundary layer. The numerical coupling of this two models have been done and the approach is original : there is no explicit need of the displacement thickness but a set of two velocities and two temperatures (one in the main nonviscous flow and one in the boundary layer) allow this coupling. First numerical experiments have shown global coherence with previous classical models in computational acoustics (characteristics, linear Kirchhoff theory). Moreover, first application to one-dimensional modelling of trombone confirm the importance of nonlinear wave propagation and in particular the "brassy" sound that is familiar to jazz musicians. The extensions of this work concern a complete treatment of nonlinear waves with precise simulation of shock waves in the trombone, new numerical experiments where convolution effects in the boundary layer are computed with direct numerical resolution of heat equation, coupling for aerodynamic flows where displacement effects play an important role (see *e.g.* Lagree [La2k]), and mathematical study of simplified models. The authors thank P.Y. Lagree for precise reading and comments on the first version of the manuscript.

10) References.

- [ABC92] B. Aupoix, J. Ph. Brazier and J. Cousteix. Asymptotic Defect Boundary-Layer Theory Applied to Hypersonic Flows, *AIAA Journal* , vol. 30, n°5, p. 1252-1259, 1992.
- [APK97] N. Amir, V. Pagneux, J. Kergomard. Wave propagation in acoustic horns through modal decomposition, in *Proceedings of the Institut of Acoustics ISMA'97*, Edimbourg, 1997.
- [Ba67] G.K. Batchelor. *An introduction to fluid dynamics*, Cambridge University Press, 1967.

- [BHKP89] M. Bruneau, P. Herzog, J. Kergomard, J.D. Polak. General formulation of the dispersion equation in bounded visco-thermal fluid ; application to simple geometries, *Wave motion*, vol. 11, p. 441-451, 1989.
- [BL78] B.S. Baldwin, H. Lomax. Thin layer Approximation and Algebraic Model for Separated Turbulent Flows, AIAA Paper n° 78-257, AIAA 16th Aerospace Sciences Meeting, Huntsville, Alabama, 1978.
- [Bl85] D.T. Blackstock. Generalized Burgers equation for plane waves, *Journal Acoust. Soc. Am.* , vol. 77, n° 6, p. 2050-2053, 1985.
- [Br97] Y. Brenier. Personal communication, april 1997.
- [Br98] M. Bruneau. *Manuel d'acoustique fondamentale*, Hermès, Paris, 1998.
- [CF48] R. Courant, K.O. Friedrichs. *Supersonic Flow and Shock Waves*. Interscience Publishers Inc., New York, 1948.
- [Ch64] W. Chester. Resonant oscillations in closed tubes, *J. Fluid Mech.*, vol. 18, p. 44-64, 1964.
- [Co88] J. Cousteix. *Couche limite laminaire*, Cepadues Editions, Toulouse, 1988.
- [DF89] F. Dubois, P. Le Floch. Boundary Conditions for Nonlinear Hyperbolic Systems of Conservation Laws, *Notes on Numerical Fluid Dynamics* (Ballmann-Jeltsch Editors), vol. 24, p. 96-104, Vieweg, 1989.
- [GM98] J. Gilbert, R. Msallam. Chocs cuivrés, *Pour la Science*, p. 27, février 1998.
- [Ha98] L. Halpern. Personal communication, april 1998.
- [He79] G.W. Hedstrom. Nonreflecting Boundary Conditions for Nonlinear Hyperbolic Systems, *J. Comput. Physics*, vol. 30, n° 2, p. 222-237, 1979.
- [HGMW96] A. Hirschberg, J. Gilbert, R. Msallam, A.P.J. Wijnands. Shock waves in trombones, *J. Acoust. Soc. Am.*, vol. 99, n° 3, p. 1754-1758, 1996.
- [KCL78] P. Kutler, S. Chakravarthy, C.K. Lombard. AIAA Paper n° 78-213, 1978.
- [Ke81] J. Kergomard, Acoustique musicale et champ interne des instruments à vent, Thèse de l'Université du Maine, Le Mans, 1981.
- [Kr70] H.O. Kreiss. Initial Boundary Value Problems for Hyperbolic Systems, *Comm. Pure Appl. Math.*, vol. 23, p. 277-298, 1970.
- [La2k] P.Y. Lagrée. An inverse technique to deduce the elasticity of a large artery, *European Physical Journal, Applied Physics*, vol. 9, p. 153-163, 2000.
- [LB80] J.C. Le Balleur. Calcul des écoulements à forte interaction visqueuse au moyen de méthodes de couplage, in Computation of viscous flow interactions, AGARD CP 291, U.S. Air Force Academy, Colorado Spring, C.O., sept.-oct. 1980.

- [Li78] J. Lighthill. *Waves in Fluids*, Cambridge University Press, 1978.
- [LL53] L. Landau, E. Lifschitz. *Fluid Mechanics*, Nauka, Moscow, 1953.
- [LW60] P.D. Lax, B. Wendroff. Systems of Conservation Laws, *Comm. Pure Appl. Math.*, vol. 13, p. 217-237, 1960.
- [MDDC97] R. Msallam, S. Dequidt, F. Dubois, R. Caussé. Modèle et simulations numériques de la propagation acoustique non-linéaire dans les conduits, Congrès of the Société Française d'Acoustique, Marseille, avril 1997.
- [MF53] P. Morse, H. Feshbach. *Methods of Theoretical Physics*, Mc Graw Hill Company, New York, 1953.
- [MG97a] L. Menguy, J. Gilbert, Congrès of the Société Française d'Acoustique, Marseille, avril 1997.
- [MG97b] L. Menguy, J. Gilbert, personal communication, 1997.
- [Ms98] R. Msallam. Modèle et simulations numériques de l'acoustique non linéaire dans les conduits ; application à l'étude des effets non linéaires dans le trombone. *Thèse de l'Université Paris 6*, december 1998.
- [MO97] S. Makarov, M. Ochmann. Nonlinear and Thermoviscous Phenomena in Acoustics, Part II, *Acta Acustica* , vol. 83, p. 197-222, 1997.
- [MT75] P. Merkli, H. Thoman. Transition to turbulence in oscillating pipe flow, *Journal of Fluid Mechanics* , vol. 68, p. 567, 1975.
- [Pi81] A.D. Pierce. *Acoustics. An introduction to its physical principles and applications*, Mc Graw Hill, New York, 1981.
- [Qu95] B. Quinnez. Modélisation des phénomènes aéroélastiques basée sur une linéarisation des équations d'Euler. Thèse de doctorat, *Ecole Centrale de Paris*, 1995.
- [RT92] S.G. Rubin, J.C. Tannehill. Parabolized Reduced Navier-Stokes Computational Techniques, *Annu. Rev. Fluid Mech.*, vol. 24, p. 117-144, 1992.
- [Sc55] H. Schlichting. *Boundary-Layer Theory*, Mac Graw Hill, New York, 1955.
- [Su91] N. Sugimoto. Burgers equation with fractional derivative ; hereditary effects on nonlinear acoustic waves, *Journal of Fluid Mechanics*, vol. 225, p. 631-653, 1991.
- [Wh74] G.B. Whitham. *Linear and nonlinear waves*, John Wiley & sons, New York, 1974.
- [Ze92] R. Zeytounian. *Modélisation asymptotique en mécanique des fluides newtoniens*, Société de Mathématiques Appliquées et Industrielles, Mathématiques et leurs applications, vol. 15, Springer Verlag, 1992.